Change in Auger Signal Intensity Caused by Surface Topography

Mineharu Suzuki[1)], Kadena Mogi, Toshio Ogino*, and Shingo Ichimura**

Center for Materials Development & Analytical Technology, NTT Advanced Technology Corporation, 3-1 Morinosato-Wakamiya, Atsugi, Kanagawa 243-01
**NTT Basic Research Laboratories, 3-1 Morinosato-Wakamiya, Atsugi, Kanagawa 243-01*
***Electrotechnical Laboratory, 1-1-4 Umezono, Tsukuba, Ibaraki 305*
E-mail: msuzuki@atsugi.ntt-at.co.jp[1)]

(Received: Jan. 30, 1997 Accepted: Feb. 20, 1997)

Abstract

Electron scattering in a well-defined comb-like structure formed on a silicon wafer was investigated to determine the effect of sub-μm to μm features in order to raise the quality of Auger electron spectroscopy (AES) analysis. Preliminary results show that the scattering becomes stronger as the line width becomes narrower. For example, the intensity from a 0.4-μm-wide line is about 1.7 that from a 1.35-μm-wide line for silicon LMM Auger transition. They also show that lower kinetic-energy electrons are more sensitive to line width in the order from secondary electron, to Si LMM, to Si KLL Auger transitions for a primary electron beam of 10 keV. There are almost no differences, however, among the three transitions for a primary electron beam of 20 keV.

1. Introduction

The scale of surface features became extremely small with the advent of very-large-scale integration (VLSI) techniques and quantum electronics. Large-scale integrated devices have been fabricated using a quarter-micrometer pattern rule. Scanning electron microscope (SEM) is widely used to observe surface features, as is scanning Auger electron microscopy (SAM). The latter currently uses a field-emission type electron gun that creates an electron beam about 10 nm in diameter, making it for both feature observation and composition analysis. When small features are observed using SEM or SAM, the signal intensity is enhanced at their edges due to the scattering caused by the electron-beam probe. This makes it difficult to quantitatively analyze and to compare the compositions of different size features.

Experimental investigations have been reported by Umbach [1] for small Au structures on Si substrates and by Hösler [2] for sidewall surfaces of LSI patterns. Experimental edge effects have been compared with theoretical investigations [3]. In these investigations, although the observed structures were formed from materials other than substrate materials, the results are still useful. The electron yields from trench structures have been simulated for SEM observations [4, 5], and a Monte Carlo simulation program has been developed for SEM imaging that can be used for small features [6]. In these simulations the primary electron beam energy was varied; however, the energy dispersion of the emitted secondary or Auger electrons was not reported.

A practical application of SAM is to observe small particles on patterns with various line widths. The observed particle composition appears to differ due to electron scattering even if the actual composition is the same. It is thus necessary to study secondary/Auger electron intensities from various-sized features made from substrate materials. In this paper, we report the preliminary experimental results for secondary/Auger electron intensity changes on a comb-like silicon pattern. The intensity from an infinite area is compared with that from the line pattern defined by a given width, whose surface is at the same level as that of the infinite area.

2. Experimental

The sample comb-like pattern was lithographically fabricated on a silicon (100) substrate; it had an infinite area on the left side and a line-and-space pattern extending to the right (Fig. 1(a)). The six line (W) and space (S) pairs (W, S) had widths of (0.4 and 0.8 μm, 0.55 and 1.13 μm, 0.8 and 1.2 μm, 1.0 and 1.44 μm, 1.175 and 1.65 μm, and 1.35 and 1.82 μm), measured using SEM. The line height (H) was 1 μm for all line patterns; the surface level of the infinite area was the same as that of the line pattern (Fig. 1(b)). One-keV Ar ion sputtering was done prior to SAM observation to remove the contaminated layer and the oxide layer

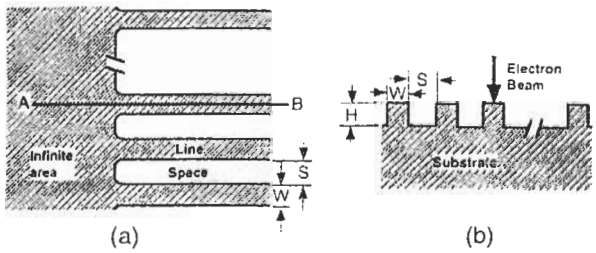

Fig. 1 (a) Top view of comb-like pattern on silicon substrate. The primary electron beam was scanned along the line AB bisecting the line pattern; W and S correspond to the width of the line and of the space, respectively. (b) Cross-sectional view from the rightside in (a); H corresponds to the height of the line pattern from the substrate.

(about 3 nm thick in total).

The SAM observations were done under a vacuum of less than 4×10^{-10} Torr by using a field-emission type Auger electron microscope (SAM670*xi*, Physical Electronics Inc.). The electron beam conditions were 10 kV and 3 nA or 20 kV and 3 nA: the corresponding beam diameters were 25 or 15 nm. The electron gun coaxially placed at the center of a cylindrical mirror analyzer; the beam hit the sample along the normal direction. The secondary electrons (SE) and Auger electrons (AE) were measured at 256 points along the line by using the intensities defined as the difference (P-B) between the peak intensity (P) and the background intensity (B). For the SE, Si LMM, and Si KLL Auger transitions, the kinetic energies (P and B) of the peak and background were (10 and 20 eV), (93.3 and 107.6 eV), and (1619 and 1634 eV), respectively. We also measured the SE and AE intensities for two lines with the same width and determined that their intensity distributions were identical.

3. Results and Discussion

The SE/AE spectra for the sputtered surface are shown in Fig. 2. The only characteristic peaks in the wide spectrum (Fig. 2(a)) are for the SE, Si LMM, and Si KLL transitions. These peaks are expanded in Fig. 2(b) and (c) to show the (P-B) intensities. The measured intensities for the 0.4 μm-wide line are shown in Fig. 3(a) as typical results. The intensities of the SE and Si LMM transition in the infinite area are almost the same. The SE intensity sharply increases at the boundary and reaches a constant value at a distance of about 3 μm, whereas the Si LMM intensity gradually increases to 6 μm (the maximum measured distance). The intensity of the Si KLL transition is constant after about 3 μm, like that of the Si SE. The distributions are converted to normalized intensity distributions in Fig. 3(b). The intensities of the SE and Si LMM start to increase at about 1.0 μm, about 0.5 μm inside the boundary; that of the Si KLL begins increasing closer to the boundary point. The normalized intensities of the Si LMM and Si KLL are almost the same at a distance of 6.0 μm, about 4.5 μm beyond the boundary. They are about twice as large as the intensity in the flat area. In the following discussion, the term "intensity" means normalized intensity.

The signal enhancements at the line patterns comparing the signal at the flat area are basically caused by electron scattering effects. The primary electrons are scattered during penetrating the line pattern and a part of scattered electrons go out from the walls of line pattern and hit the bottom surfaces of the space region. These electrons excite SE and AE at the walls and the bottom of the space. Another excitation of SE/AE takes place at the bottom by backscattered electrons. The electrons

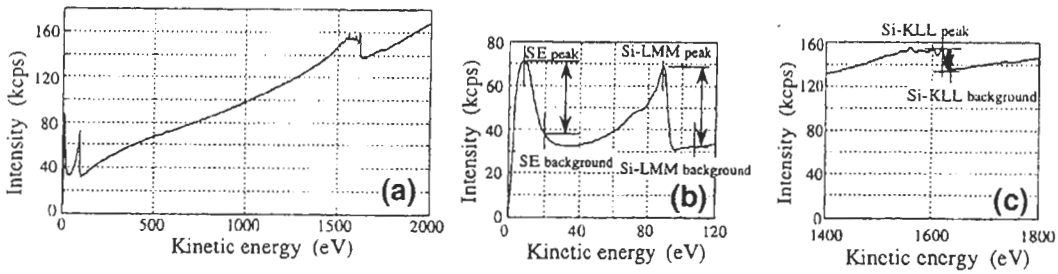

Fig. 2 Secondary electron (SE) and Auger electron (AE) spectra in the infinite area; the primary electron beam had an energy of 10 keV. (a) Wide-range spectrum of kinetic energy, from 0 to 2000 eV. (b) Spectrum covering SE and Si LMM peaks from 0 to 120 eV. The peak and background positions are noted and their differences are defined as the peak intensities. (c) Spectrum covering Si KLL peak from 1400 to 1800 eV. The peak intensity corresponds to the difference between the local maximum position at the higher kinetic energy and the background position.

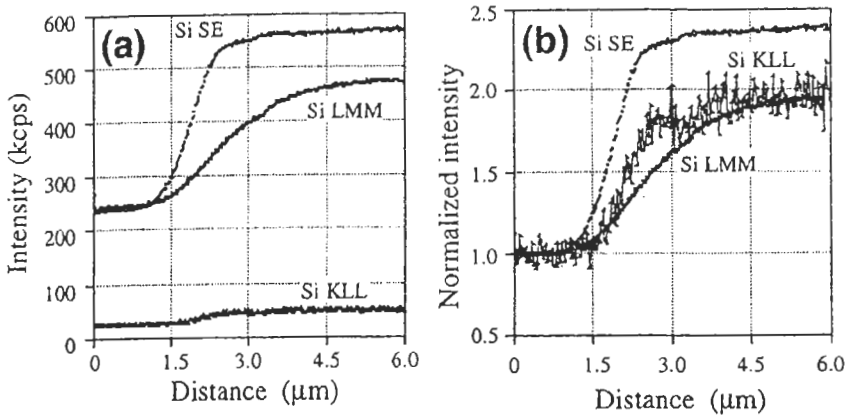

Fig. 3 (a) Peak intensity distribution along the 0.4-μm-wide line; the primary electron beam had an energy of 10 keV. The horizontal axis corresponds to the scanning distance along the bisecting line. The origin is in the infinite area, and the position at 1.5 μm corresponds to the boundary between the flat area and the line region. The vertical height is the intensity, which is the counted number of electrons (P-B). (b) Normalized intensity distribution along the 0.4-μm-wide line. The average value of 20 points in the range from about 0.5 to 1.0 μm in Fig. 3(a) are normalized to unity.

generated by various kinds of scattering cause the signal enhancement at the line pattern. The intensity distribution around the boundary is different between SE, Si LMM, and Si KLL as mentioned above. This may be because the information depths determined by inelastic mean free paths are different at the kinetic energies of SE/AE transitions.

The Si KLL intensity does not change over the entire distance of the 1.35-μm-wide line for the primary beam of 10 keV, although the three intensity distributions are not shown here. The Si KLL intensity is sensitive to the line width and is obviously affected by widths narrower than 1.0 μm. Generally speaking, the intensity is strong in the order of SE, Si LMM, and Si KLL for a primary electron beam energy of 10 keV. For a beam energy of 20 keV, the intensities of these three peaks show the same behavior up to 6 μm, reaching the same value at 6 μm.

Figure 4 shows the Si LMM intensity distributions for all of the tested line widths with primary electron beam energies of 10 and 20 keV. For both energies, the intensity at a line is stronger when the line is thinner. At 10 keV the intensities between 1.5 and 3.0 μm are inverted for line widths of 0.8 and 1.0 μm, probably because the actual topographic shapes from the infinite area to the line region at the boundary are not similar. At 20 keV the intensity distributions begin increasing at the origin, meaning that the electron scattering is affected even at a position 1.5 μm inside the boundary. The shoulder structure at about 3.0 μm for the 0.4-μm-wide line is because there was a small particle (maybe silicon) on the sidewall at this position that was observed with SEM. The intensity difference is obviously large between the 0.4- and 0.55-μm-wide lines,

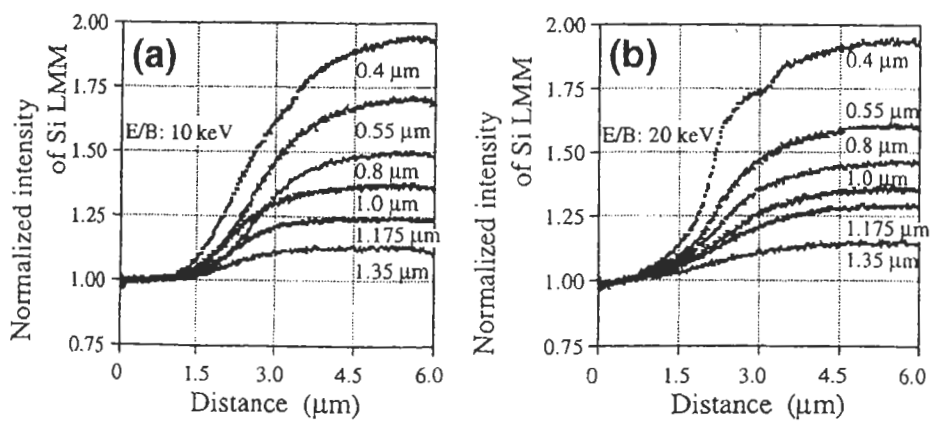

Fig. 4 Line-width dependence of Si LMM intensity for primary electron beam energies of (a) 10 and (b) 20 keV.

comparing the differences between other wider lines. Although the electron scattering from this kind of structure needs to be studied using theoretical simulation in order to clarify the factors causing the scattering, there is apparently a critical line width at around 0.5 μm for electron scattering.

Figure 5 shows the SE intensity distributions for primary electron beam energies of 10 and 20 keV. The behaviors are very similar to those for Si LMM (Fig. 4). The problems caused by the topographic shapes at the boundary for the 0.8 - and 1.0-μm-wide lines and by the small particle on the sidewall again occur. The intensity differences at 6.0 μm between the 10-keV- and that for the 20-keV-primary beams are greater than those for the Si LMM. This indicates that electrons with a kinetic energy of about 10 eV, corresponding to the SE, are more sensitive to the topography than electrons with the kinetic energy of about 90 eV, corresponding to the Si LMM transition.

So far we have discussed the results depending on the primary beam energy and on the line width independently. Fig. 6 shows the intensity distributions depending on both factors for SE (Fig. 6(a)) and Si LMM (Fig. 6(b)) electrons. For lines of any width, the SE intensity created by a primary electron beam of 10 keV is greater than that of a 20-keV beam. The difference in SE intensities between 10- and 20-keV electron beams increases with a decreasing line width. Figure 6(b) shows that the intensity distributions do not depend on the primary electron beam. The intensities start to increase at about 1.0 μm (0.5 μm inside the boundary) and reach constant values at 4.0 to 4.5 μm for the Si LMM Auger electrons. The transient distance is shorter for SEs (kinetic energy of 10 eV) than for Si LMM AEs (kinetic energy of 93 eV); the difference is in the μm range. This might be because the inelastic mean free path of electrons for 10-eV-electrons is several times greater than that for 93-eV electrons [7]. Further investigation, especially using theoretical simulation, is needed to clarify this

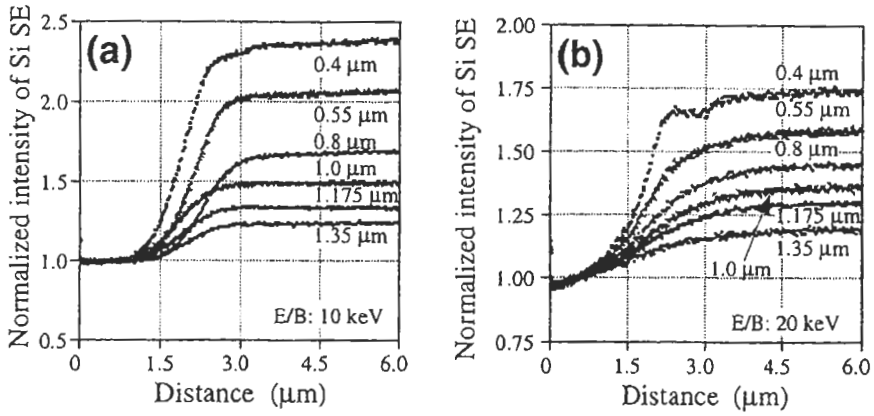

Fig. 5 Line-width dependence of Si SE intensity for primary electron beam energies of (a) 10 and (b) 20 keV.

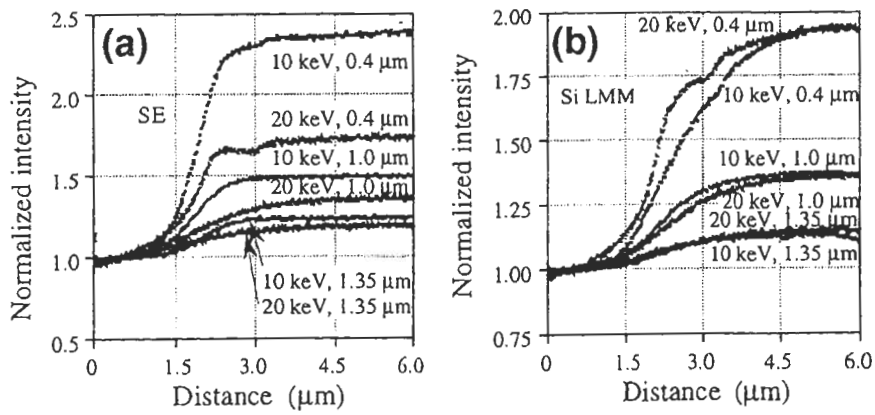

Fig. 6 (a) Intensity distributions for SE depending on the primary beam energies and line widths. The primary beam energy was 10 or 20 keV, and the line width was 0.4, 1.0, or 1.35 μm. (b) Intensity distributions for Si LMM electrons depending on the primary beam energies and line widths. The primary beam energy was 10 or 20 keV, and the line width was 0.4, 1.0, or 1.35 μm.

result.

Figure 7 shows the saturated intensity on a line (e. g., from 5.53 to 6.0 μm along the horizontal axis in Fig. 6) for primary electron beam energies of 10 and 20 keV. Two values are plotted at each line width for each transition (SE, LMM, and KLL); in each case the two symbols almost overlap. At 10 keV, however, SE had a large relative intensity and KLL has a small one. The LMM transition is close to that of KLL in the narrow-line-width region, while it is close to that of SE in the wide-line-width region. The intensity dispersion at a given line width is very small for the three transitions at a primary beam energy of 20 keV, although the intensity for the 0.4-μm line width is as large as 1.5 times that for the 1.35-μm line width.

Our results show that composition analysis to measure a wide kinetic-energy range should be done using a higher-energy primary beam. While it is difficult to compare analytical results for different line widths, even when using higher-primary beam energy, it should become possible to perform quantitative analysis using numerical processing after further experimental investigation, including reproducibility, and after theoretical simulation with the SE/AE transition, the line width, and the primary beam energy used as parameters. Theoretical simulation is needed to analyze the scattering effect due to excitations separated from intensities at a top surface, at a side wall, and at a bottom surface in a space region.

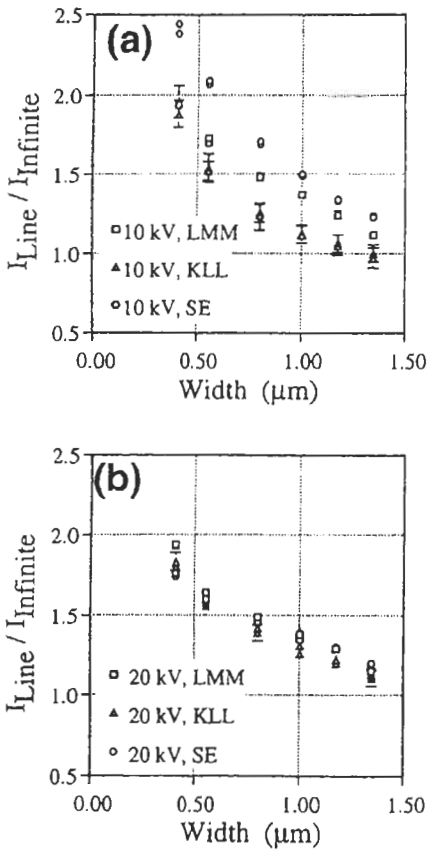

Fig. 7 Saturated intensity on lines normalized by intensity in the infinite area, as averaged for 20 points in the range from 5.53 to 6.0 μm (a) primary electron beam energies of 10 and (b) 20 keV.

4. Summary

We have investigated electron scattering in a well-defined comb-like structure formed on a silicon wafer to determine the effect of sub-μm to μm features on the electron beam in order to raise the quality of AES quantitative analysis. The signal intensities were defined as the differences between the peak intensities and background intensities for SE (secondary electron), Si LMM, and Si KLL Auger transitions. We found that the scattering is stronger the narrower the line. For example, the intensity from a 0.4-μm-wide line is about 1.7 times that from a 1.35-μm-wide line for Si LMM. In the infinite area, the intensity distribution was affected by the comb-like structure at a point 0.5 μm inside the boundary for a 10-keV primary beam and at a point 1.5 μm inside the boundary for a 20-keV primary beam. Lower kinetic-energy electrons were found to be more sensitive to line width in the order of SE, to Si LMM, to Si KLL transitions for a primary electron beam of 10 keV. There are almost no differences, however, among the three transitions for a primary electron beam of 20 keV.

Acknowledgments

We are indebted to Professor Masatoshi Kotera of the Osaka Institute of Technology for his useful discussions.

References

1. A. Umbach, A. Hoyer, and W. H. Brünger, Surf. Interface Anal. **14**, 401 (1989).
2. W. Hösler, Surf. Interface Anal. **17**, 543 (1991).
3. M. M. El Gomati, M. Prutton, B. Lamb, and C. G. Tuppen, Surf. Interface Anal. **11**, 251 (1988).
4. Masatoshi Kotera, Satoru Yamaguchi, Sachio Umegaki, and Hiroshi Suga, Jpn. J. Appl. Phys. **32**, 6281 (1993).
5. Masatoshi Kotera, Satoru Yamaguchi,

Sachio Umegaki, and Hiroshi Suga, Jpn. J. Appl. Phys. **33**, 7144 (1994).
6. David C. Joy, Microbeam Analysis **4**, 125 (1995).
7. M. P. Seah and W. A. Dench, Surf. Interface Anal. **1**, 2 (1979).